Vapour pressure measurements of liquid heavy water in the temperature range between 256 K and 286 K

(Article begins on next page)

VAPOR PRESSURE MEASUREMENTS OF LIQUID HEAVY WATER IN THE TEMPERATURE RANGE BETWEEN 256 K AND 286 K

Authors: G. Beltramino, L. Rosso, R. Cuccaro, V. Fernicola

Affiliation: INRIM - Istituto Nazionale di Ricerca Metrologica, Torino, Italy

Corresponding author: R. Cuccaro (*r.cuccaro@inrim.it*)

Abstract

The thermodynamic properties of heavy water (D_2O) are of interest in the industrial field as well as the scientific domain, both on the application side and for the understanding of isotopic effects in aqueous solutions.

In contrast with ordinary water (H_2O), comparatively few saturation vapor pressure measurement data of D_2O are reported in the literature in the temperature range in which heavy water is at its supercooled state, sometimes with limited or unknown measurement uncertainty.

To fill for the lack of experimental data, in this work accurate measurements of the vapor – liquid equilibrium along the saturation line of heavy water over the temperature range from 256 K to 286 K are performed, so including a wide subrange where heavy water is kept at the supercooled state (256 K – 277 K).

A comparison between the experimental measurements performed in this work and the available literature data is carried out along with the recent D_2O vapor pressure formulation. Measurement results are discussed and uncertainty sources are estimated.

Keywords: Supercooled heavy water; Saturation vapor pressure; Capillary tube; Water vapor properties

1. Introduction

Deuterium oxide (D_2O) or heavy water is a substance of commercial and scientific interest. Liquid heavy water is used as neutron moderator into the nuclear reactors; recently, it has gained importance in the biological and medical field in the so-called boron neutron capture therapy, an emerging helpful tool in treating cancer [1].

The accurate determination of its thermodynamic properties is of great importance for the evaluation of the isotope effects on the physical properties of water and aqueous solutions. In particular, the measurement of the saturation vapor pressure of D_2O provides information about the vapor pressure isotope effect (VPIE), useful for the understanding of the nature of intermolecular forces in condensed phases.

In the last decade the thermodynamics of ordinary water (H_2O) has been the subject of many studies, resulting in the availability of accurate experimental data and formulations over a broad temperature range. Nonetheless, a limited number of data of saturation vapor pressure of supercooled liquid water is reported in literature, often without a clear uncertainty assessment. For supercooled D_2O, available data are fewer than for H_2O. Moreover, currently a thermodynamic integration approach to the supercooled vapor pressure of D_2O is not possible due to the lack of high-accuracy triple-point pressure knowledge.

Most of the experimental data available in literature [2-15] concerns the saturation vapor pressure of stable liquid D_2O, which is often reported as difference or ratio with respect to ordinary water. It is worth mentioning the first saturation vapor pressure data provided in the '30s by Lewis and MacDonald [8] and Miles and Menzies [9]. Lewis and MacDonald carried out measurements of heavy water vapor pressure from 293 K up to 389 K and were probably the first to report the boiling and freezing points of D_2O. Miles and Menzies extended the investigated temperature range up to 502 K, finding the crossover point of the saturation vapor pressure curves of the two water isotopes at about 497 K.

The temperature at which the vapor pressures of heavy and ordinary water coincide was determined more accurately by Oliver and Grisard [11] in 1956, who also published the most reliable data between 495 K and the D_2O critical temperature ($T_c = 643.847$ K) used for the validation in this temperature range of the current reference equation of state (EOS) for heavy water.

Also Zieborak's [14] experimental data published in 1966 were used for the equation of state (EOS) validation between 350 K and 495 K, while vapor pressure data provided by Besley and Bottomley [3] in 1973 were used for the fitting in the range between the triple point and 300 K.

To the author's knowledge, the latest saturation vapor pressure measurements were carried out by Jákli and Markó in 1995 in the temperature range between 281 K and 353 K and reported in the publication of Harvey and Lemmon [16] with the permission of the authors.

Concerning saturation vapor pressure of heavy water in the metastable supercooled liquid region, available data are sparse. Only three authors report measurements in this region. Pupezin *et al.* [2] reported measurements of vapor pressure from 273 K to 372 K,

providing data for D_2O supercooled state just below its melting point. Bottomley [6] investigated the temperature range between 261 K and 276 K, while Kraus and Greer [7] extended the investigated range down to 257 K.

Based on available measurements, several D_2O saturation vapor pressure formulations were developed in the past years [2-3, 16-22]. Many of these equations correlate the vapor pressure to the temperature via functional form with constants determined by the least-squared method on available experimental data. Considering the limited data available in the supercooled region, formulations usually refer to temperature ranges above the melting point.

The range of validity of the current reference EOS for the thermodynamic properties of the fluid phases of D_2O, also known as IAPWS R16-17 [23], is officially limited to stable states at temperatures above the lowest temperature on the melting-pressure curve up to 825 K at pressures up to 1200 MPa. It does not cover the metastable supercooled liquid region, even if the formulation behaves reasonably when extrapolated into this region. This equation, developed by Herrig *et al.* [21], has been adopted by the International Association for the Properties of Water and Steam (IAPWS) in 2018, replacing the previous reference EOS published by Hill *et al.* [22] in 1982. Both formulations are explicit in the Helmholtz free energy, a, as a function of density, ρ, and temperature, T. All thermodynamic properties of the fluid including saturation vapor pressure can be derived by combining derivatives of the functional form $a(T,\rho)$ of the equation or its dimensionless function $\alpha(\tau,\delta) = a(T,\rho)/(RT)$, where R is the molar gas constant, $\tau = T_c/T$ and $\delta = \rho/\rho_c$ with T_c and ρ_c temperature and density at the critical point respectively.

With regards to the saturation vapor pressure formulations, the equations suggested by Jancso and Van Hook [17] and the functions for their own data provided by Pupezin *et al.* [2], by Bottomley [6] and Kraus and Greer [7] are among the few whose validity extends to D_2O supercooled region. The formulations suggested by Jancso and Van Hook and by Pupezin *et al.* are recommended in the temperature range from 268 K to 353 K, while that one of Bottomley cover the range between 261 K and 276 K.

To fill for the lack of experimental data in the supercooled region, new accurate saturation vapor pressure measurements of liquid heavy water, over the temperature range from 256 K to 286 K, were carried out at the Istituto Nazionale di Ricerca Metrologica (INRIM). In this work measurement results and the corresponding uncertainty analysis are provided. Experimental data are also compared with those available in literature and with some of the most recent D_2O saturation vapor pressure formulations.

2. Experimental and data analysis techniques

The saturation vapor pressure of D_2O is determined by measuring the static pressure that originates inside a closed volume when the liquid and the vapor phases of the fluid are at the equilibrium. According to the Gibbs phase rule, the value of the saturation vapor pressure depends exclusively on the temperature at the liquid-vapor interface of the sample under investigation.

In the present work, measurements are carried out on commercial heavy water samples with an isotopic purity of 99.9 atomic % D produced by Sigma-Aldrich.

A detailed description of the experimental apparatus used in this work and depicted in Figure 1 can be found in a previous work of Beltramino *et al.* [23]. The set-up, which was previously used for the measurement of the saturation vapor pressure of ordinary water, consists of: a sample cell in the form of a U-shaped capillary tube made of borosilicate-glass with a 6-mm outer diameter and a 0.4-mm inner diameter; a stainless steel cylindrical cell used as the heavy water reservoir for the filling of the sample cell; a differential manometer; a valve manifold for the connection of both cells to the manometer and to a turbo-molecular vacuum pump (TMP). A thermostatic liquid bath filled with ethanol hosts the sample cells.
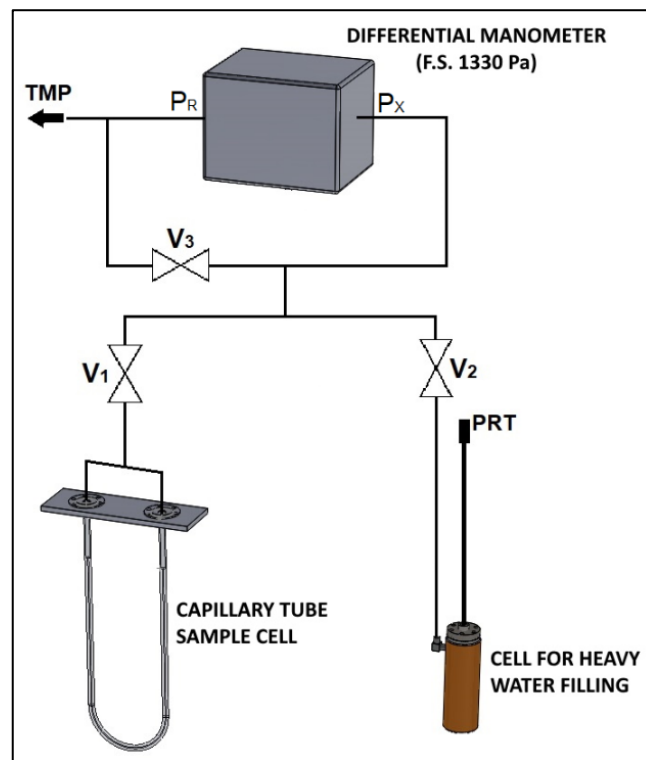
Figure 1. Experimental apparatus for the measurement of the saturation vapor pressure of liquid heavy water. PRT – platinum resistance thermometer; TMP – turbo-molecular pump; P_R – reference pressure for the differential manometer; P_X – pressure in the system; V_1 – valve to sample cell; V_2 – valve to cell for heavy water filling; V_3 – valve to TMP.

An important preliminary step in the preparation of the experiment is the filling of the capillary tube with a D_2O sample. The filling procedure plays an important role for reducing the entrance of ambient air, thus avoiding any contamination of the sample with ordinary water present in the atmosphere, and for minimizing the risk of particulate and dust deposition on the internal wall of the sample cell. Both phenomena limit downward the temperature at which the sample can be maintained at the supercooled liquid state.
The D_2O transfer from the original glass bottle to the cylindrical cell was performed in a dry atmosphere by flowing dry nitrogen in the area around the cell. The latter was filled with about 55 ml of D_2O, a sufficient amount of heavy water to complete the whole experiment without a further exposition of the sample at the ambient air for a refill.

Once filled up, the cylinder was immersed in the thermostatic bath at a temperature of about 263 K, to freeze the sample. Valves V_2 and V_3 are open and the ambient air entered in the experimental apparatus during the transfer of the sample is pumped out using the TMP. Afterwards, valve V_3 is closed and the cell is allowed to warm to a room temperature of about 298 K, while the bottom of the capillary tube is kept immersed in the bath at 263 K. The sample cell, previously evacuated, is then connected to the cylindrical cell by opening valve V_1.

The water vapor evaporated from the liquid D_2O in the reservoir partially condensates on the sample cell walls, thus resulting in a transfer to the sample cell. Finally, valve V_2 is closed and the D_2O in the sample cell subjected to a further degassing process, as described in Beltramino *et al.* [24]. Such filling procedure, resulting in a small amount (< 1 ml) of heavy water in the capillary tube, and degassing process were essential steps for achieving and maintaining the sample at the supercooled liquid state down to 256 K. Once the sample preparation was completed, the capillary tube was isolated from the system by means of valve V_1 and the whole system was carefully evacuated to reach a residual pressure equal to or lower than 10^{-4} Pa. The sample cell was then fully immersed in the thermostatic bath, the connection via the manifold valve was re-established and, once a liquid-vapor equilibrium was attained, the measurements of the vapor pressure were carried out.

Three measurement runs of the D_2O saturation vapor pressure were performed in the temperature range from 256 K to 286 K. The lowest temperature corresponds to a consistent supercooled liquid state of the sample throughout the experiments. Each measurement run consisted of 31 pressure values determined measuring the vapor pressure at temperature steps of 1 K, starting from the lowest temperature. Between each run, the sample cell was isolated from the manometer and the system evacuated in order to check for any drift of the manometer which was zeroed when required.

Each measurement step lasted four or five hours, of which about two hours were taken to equilibrate the vapor pressure after a vacuum pumping [24].

Once the temperature-pressure equilibrium was attained, a steady increase of the pressure of about 30-40 mPa·h^{-1} was observed (see Figure 2). The measured system leakage was consistent with the vacuum leak specifications of the system components. To compensate for such leak, the saturation water vapor pressure was estimated by means of a linear back-extrapolation of the measured pressure to the initial time t_0, that is the time at which the sample cell is connected to the system by opening valve V_1 after an evacuation cycle.
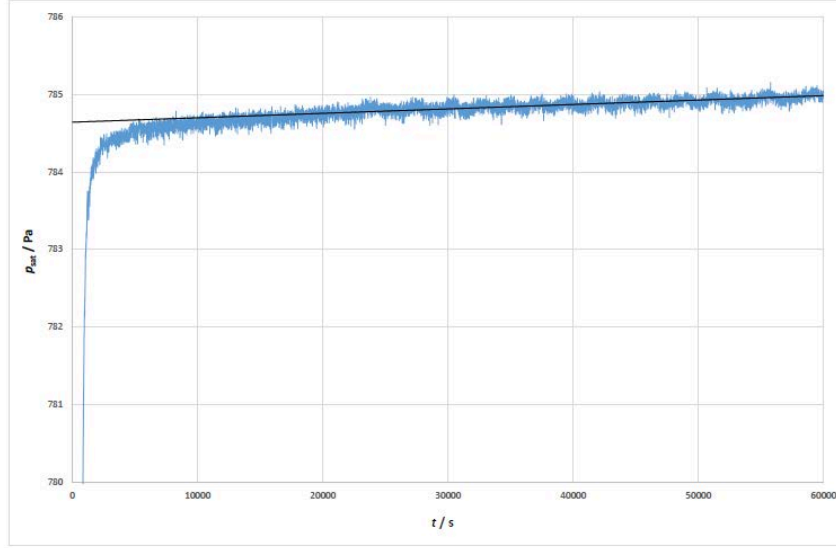
Figure 2. Details of the measurement of the saturation water vapor pressure, p_{sat}, as a function of the time, t, at the temperature $T = 279$ K. Time $t_0 = 0$ s corresponds to the connection of the sample cell to the pressure gauge via valve V₁. The liquid - vapor equilibrium is reached in about two hours. Afterwards, the slight slope of the pressure is due to a residual gas leakage in the system.

The temperature of the sample under investigation was measured by using a calibrated 100-Ω platinum resistance thermometer (PRT), traceable to ITS-90. The PRT was placed into a thermowell inside the cylindrical reservoir cell at a depth so that its sensing element was aligned with the liquid-vapor interface in the capillary. Pressure measurements were carried out by means of a differential manometer calibrated against the INRIM pressure reference standard and corrected for the manometer calibration, for the hydrostatic head and the thermal transpiration effect [24].

A correction for the sample purity was applied as follows. Given the isotopic purity specified by the producer of 99.9 atomic % D, it was supposed that sample liquid was approximately 99.8 % D₂O molecules, 0.2 % HDO molecules and a tiny number of H₂O molecules.

Considering negligible the amount of ordinary water molecules, the correction was determined by taking into account the Dalton's and the Raoult's laws for a binary mixture. The sample measured pressure, p_{meas}, i.e. the total pressure exerted by the gas mixture, can be expressed as:

$$p_{\text{meas}} = p_{\text{D}_2\text{O}} + p_{\text{HDO}}, \tag{1}$$

where p_{D2O} and p_{HDO} are the partial pressures of heavy water and semiheavy water, respectively. In addition, on the basis of Raoult's Law and considering the sample as an ideal mixture of liquids, the partial pressure of each component is equal to the vapor pressure of the pure component multiplied by its mole fraction in the mixture, that is:

$$p_{\text{D}_2\text{O}} = X_{\text{D}_2\text{O}} \times p^o_{\text{D}_2\text{O}}$$
$$p_{\text{HDO}} = X_{\text{HDO}} \times p^o_{\text{HDO}}, \tag{2}$$

where X_{D2O} and X_{HDO} are the mole fractions and $p^o{}_{D2O}$ and $p^o{}_{HDO}$ are the vapor pressures of pure heavy water and pure semiheavy water, respectively.

Combining equations 1 and 2 with the constraint $X_{D2O} + X_{HDO} = 1$ and assuming that the effective vapor pressure of HDO, which is unknown, is the mean of those of D_2O and H_2O [$p^o{}_{HDO} = (p^o{}_{D2O} + p^o{}_{H2O})/2$], the vapor pressure of pure D_2O can be expressed as follows:

$$p^o_{D_2O} = \frac{2\,p_{meas}}{X_{D2O}+1} + p^o_{H_2O} \times \frac{X_{D_2O}-1}{X_{D_2O}+1} \tag{3}$$

where the vapor pressure of pure ordinary water, $p^o{}_{H2O}$, was determined by using the IAPWS G12-15 formulation [25] and X_{D2O} was set to 0.998.

The corrections applied to raw pressure data at the corresponding temperature values are shown in Figure 3.
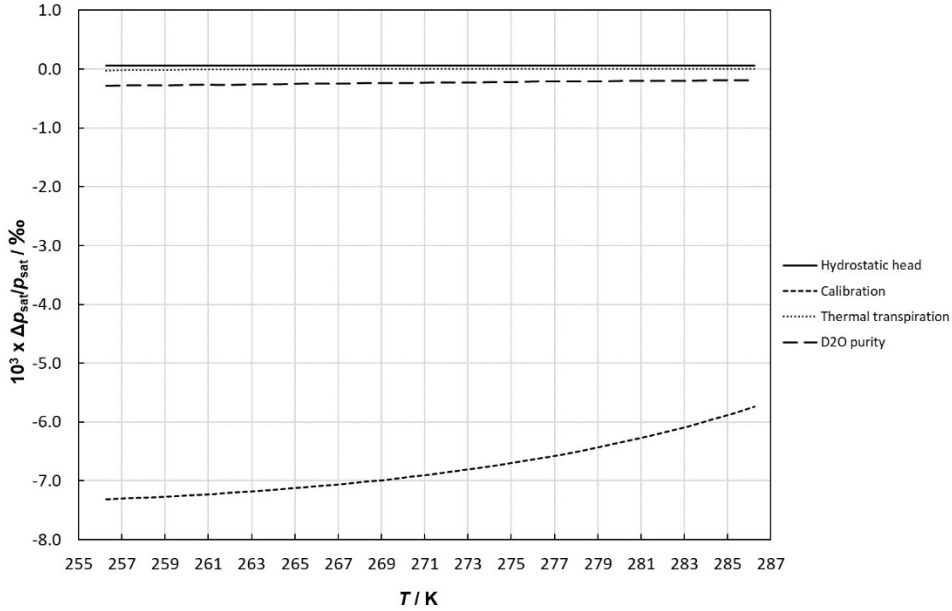
Figure 3. Corrections applied to the raw heavy water saturation vapor pressure data. The corrections account for the hydrostatic head effect, the pressure gauge calibration, the thermal transpiration effect and the purity of the investigated D_2O sample.

It's worth noting that over the whole temperature range the sample purity correction contributed to 0.02 % to 0.03 % of the pressure reading, representing a significant correction of the measured pressure.

3. Results and discussion

The corrected values of D_2O saturation vapor pressure, p_{sat}, over the temperature range from 256 K to 286 K are reported in Table I along with the expanded (coverage factor $k = 2$) combined uncertainty of the temperature $U_c(T)$ and the expanded ($k = 2$) combined

uncertainty of the saturation vapor pressure $U_c(p_{sat})$. The latter varies from 0.23 Pa at $T = 256$ K to 0.85 Pa at $T = 286$ K.

Table I. Temperature, T, and corresponding heavy water saturation vapor pressure, p_{sat}. The reported pressure values are corrected for the hydrostatic head effect, the pressure gauge calibration, the thermal transpiration effect and the sample purity. The expanded ($k = 2$) combined uncertainty of the temperature, $U_c(T)$, and the expanded ($k = 2$) combined uncertainty of the vapor pressure, $U_c(p_{sat})$, are reported as well. Different measurement runs are labeled with letters from A to C. An asterisk marks values corresponding to supercooled D_2O.

A)	T / K	$U_c(T)$ / K	p_{sat} / Pa	$U_c(p_{sat})$ / Pa
*	256.270	0.006	126.70	0.23
*	257.263	0.006	138.21	0.23
*	258.258	0.006	150.48	0.23
*	259.259	0.006	164.10	0.23
*	260.262	0.006	178.30	0.24
*	261.258	0.006	193.90	0.24
*	262.260	0.006	210.80	0.24
*	263.257	0.006	228.78	0.25
*	264.252	0.006	248.22	0.25
*	265.255	0.006	269.18	0.26
*	266.253	0.006	291.63	0.26
*	267.251	0.006	316.01	0.27
*	268.247	0.006	341.64	0.28
*	269.246	0.006	369.36	0.29
*	270.253	0.006	399.44	0.30
*	271.249	0.006	431.21	0.31
*	272.243	0.006	465.44	0.32
*	273.238	0.006	502.02	0.33
*	274.230	0.006	540.78	0.34
*	275.230	0.006	582.52	0.36
*	276.236	0.006	627.60	0.36
	277.233	0.006	674.86	0.38
	278.234	0.006	725.70	0.40
	279.233	0.006	779.49	0.44
	280.234	0.006	837.34	0.48
	281.229	0.006	898.30	0.52
	282.233	0.006	964.03	0.58
	283.233	0.006	1032.99	0.63
	284.235	0.006	1107.53	0.70
	285.233	0.006	1185.35	0.77
	286.232	0.006	1268.80	0.85

B)	T / K	$U_c(T)$ / K	p_{sat} / Pa	$U_c(p_{sat})$ / Pa
*	256.260	0.006	126.23	0.23
*	257.263	0.006	138.11	0.23

8

*	258.258	0.006	150.53	0.23
*	259.259	0.006	164.02	0.23
*	260.255	0.006	178.43	0.24
*	261.258	0.006	194.20	0.24
*	262.259	0.006	210.70	0.24
*	263.256	0.006	228.61	0.25
*	264.246	0.006	248.09	0.25
*	265.249	0.006	269.16	0.26
*	266.248	0.006	291.40	0.26
*	267.246	0.006	315.76	0.27
*	268.242	0.006	341.51	0.28
*	269.242	0.006	369.30	0.29
*	270.250	0.006	399.14	0.30
*	271.247	0.006	431.16	0.31
*	272.246	0.006	465.54	0.32
*	273.239	0.006	502.05	0.33
*	274.231	0.006	540.80	0.34
*	275.229	0.006	582.55	0.36
*	276.229	0.006	626.98	0.36
	277.232	0.006	674.70	0.38
	278.231	0.006	725.31	0.40
	279.230	0.006	779.44	0.44
	280.232	0.006	837.00	0.48
	281.229	0.006	898.07	0.52
	282.233	0.006	963.98	0.58
	283.231	0.006	1033.08	0.63
	284.232	0.006	1106.91	0.70
	285.231	0.006	1185.52	0.77
	286.230	0.006	1268.58	0.85

C)	T / K	$U_c(T)$ / K	p_{sat} / Pa	$U_c(p_{sat})$ / Pa
*	256.255	0.006	126.54	0.23
*	257.253	0.006	138.22	0.23
*	258.248	0.006	150.28	0.23
*	259.249	0.006	163.76	0.23
*	260.252	0.006	178.38	0.24
*	261.248	0.006	193.80	0.24
*	262.250	0.006	210.90	0.24
*	263.246	0.006	228.84	0.25
*	264.242	0.006	248.29	0.25
*	265.246	0.006	269.88	0.26
*	266.244	0.006	292.03	0.26
*	267.242	0.006	315.88	0.27
*	268.238	0.006	341.92	0.28
*	269.239	0.006	369.49	0.29
*	270.247	0.006	399.54	0.30
*	271.245	0.006	431.36	0.31
*	272.246	0.006	465.37	0.32
*	273.248	0.006	502.13	0.33
*	274.241	0.006	540.62	0.34
*	275.242	0.006	582.66	0.36

*	276.245	0.006	627.07	0.36
	277.243	0.006	675.19	0.38
	278.245	0.006	725.55	0.40
	279.243	0.006	779.34	0.44
	280.246	0.006	837.28	0.48
	281.241	0.006	898.12	0.52
	282.247	0.006	963.98	0.58
	283.244	0.006	1032.90	0.63
	284.245	0.006	1106.81	0.70
	285.245	0.006	1185.61	0.77
	286.244	0.006	1269.10	0.85

The combined standard uncertainty of the temperature, $u_c(T)$, estimated approximately 3 mK, results fairly constant over the whole investigated temperature range. Table II reports the sources of uncertainty considered and the respective contributions estimated referring to the worst case observed in the T range.

Table II. Standard uncertainty contributions, $u(T)$, and combined standard uncertainty, $u_c(T)$, of temperature measurements. Reported contributions refer to the worst case observed in the whole investigated T range.

Source of uncertainty	$u(T)$ / mK
Resistance Bridge Linearity	3.0
Meas. Repeatability (incl. Bath Stability)	1.1
Bath Temperature Uniformity	0.8
SPRT Calibration	0.2
Combined standard uncertainty, $u_c(T)$	3.3

Concerning the saturation vapor pressure measurement, its combined standard uncertainty, $u_c(p_{sat})$, varies from 113.0 mPa at 256 K to 426.5 mPa at 286 K. In Table III considered sources of uncertainty and respective contributions to $u_c(p_{sat})$ in terms of saturation vapor pressure standard uncertainty, $u(p_{sat})$, are reported. The main contribution comes from the manometer calibration followed by the combined temperature uncertainty, whose input to $u_c(p_{sat})$ is determined multiplying $u_c(T)$ by the sensitivity coefficient dp_{sat}/dT calculated from the EOS developed by Herrig *et al.* [21]. For temperature above 262 K, the application of the D_2O purity correction represents the third significant contribution to the saturation vapor pressure uncertainty, while below 262 K it is given by the procedure of linear back-extrapolation described previously in text.

The uncertainty contribution due to the D_2O purity correction is evaluated assuming that the measurement capabilities of the producer of the sample is at least twice better than the last significant digit used to declare the isotopic purity of the sample. Thus an uncertainty of 0.05% is assumed on the mole fraction X_{D2O}.

The uncertainty of the D₂O purity correction, $u(p^o_{D2O}-p_{meas})$, is then determined multiplying the uncertainty of the heavy water mole fraction, $u(X_{D2O})$, by the sensitivity coefficient, $d(p^o_{D2O} - p_{meas})/dX_{D2O}$, obtained from equation 3.

Table III. Combined standard uncertainty of heavy water saturation vapor pressure, $u_c(p_{sat})$, at the measurement range extremes. Sources of uncertainty and respective contributions to saturation vapor pressure standard uncertainty, $u(p_{sat})$, are reported.

Source of uncertainty	$p_{sat} \approx 127\,Pa$ $T = 256\,K$ $u(p_{sat})$ / mPa	$p_{sat} \approx 1269\,Pa$ $T = 286\,K$ $u(p_{sat})$ / mPa
Manometer calibration	102.5	323.0
Temperature uncertainty ($u_c(T) \times dp_{sat}/dT$)	33.3	270.1
D₂O purity correction	9.2	59.6
Extrapolation to time zero	32.5	32.5
Gage Zero&Span Drift (4 ppm F.S./day)	3.1	3.1
Thermomolecular Effect Correction	2.8	2.8
Hydrostatic Head Correction	0.1	0.4
Residual Gases Effect	0.3	0.3
Combined standard uncertainty, $u_c(p_{sat})$	113.0	426.5

Heavy water saturation vapor pressure experimental results of the three measurement runs are shown in Figure 4, where they are plotted as difference in pressure, Δp_{sat}, with respect to the IAPWS R16-17 formulation used as reference. For the sake of clarity, only the uncertainty bars for the first measurement run are shown. It is worth noting that values from different runs results consistent within their uncertainty and in agreement with the IAPWS R16-17 formulation.
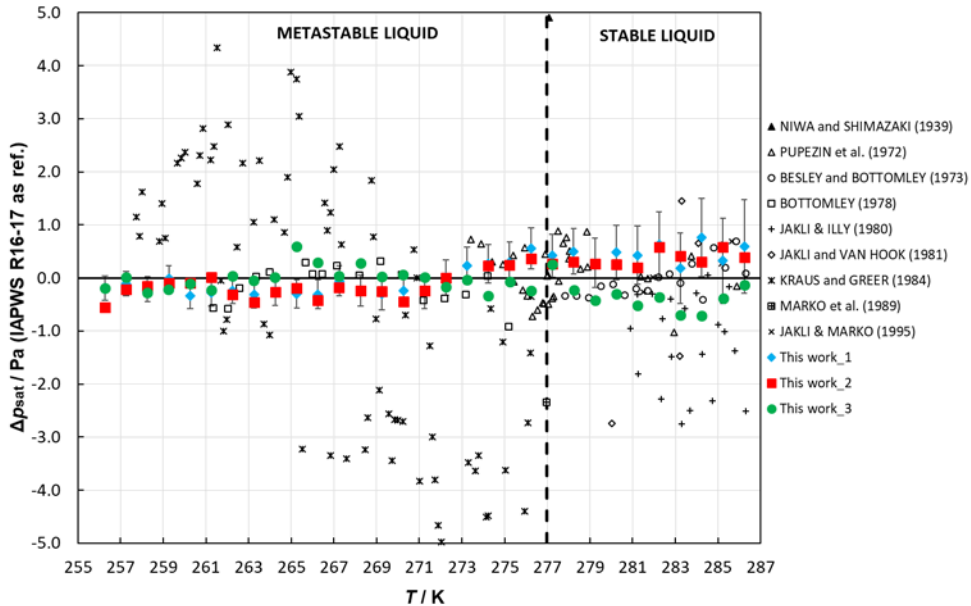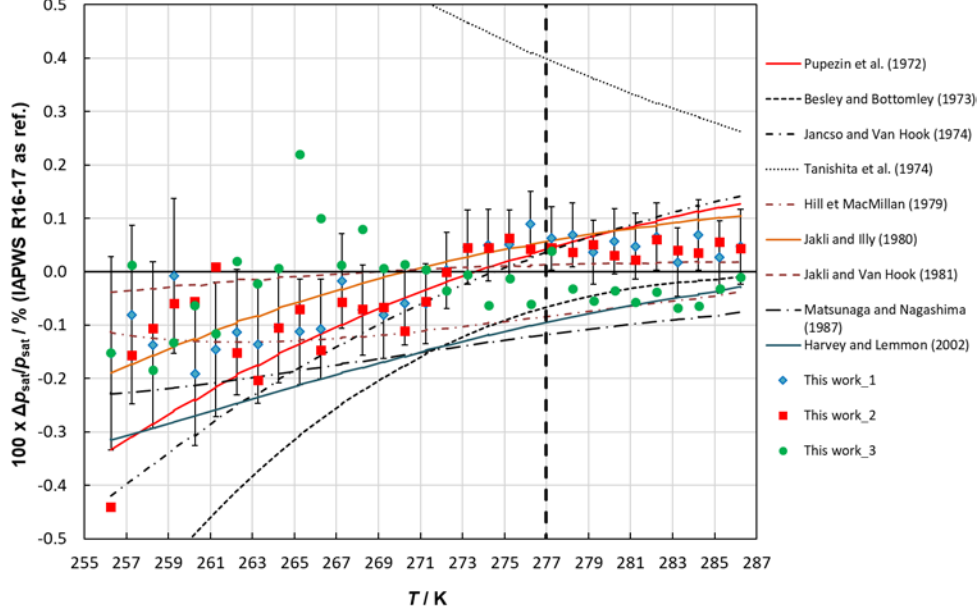
Figure 4. Comparison between the saturation vapor pressure measurements in this work and those available in the literature. All data are plotted as pressure difference, Δp_{sat}, with respect to the IAPWS R16-17 formulation, used as reference. Experimental values of this work (run 1) are plotted together with the expanded combined measurement uncertainty ($k = 2$). The dashed black line separates the metastable liquid region and the stable liquid one.

In Figure 4, measurement values obtained in this work are also compared with data available in literature [2-7, 13, 15]. As previously observed, few authors report D_2O saturation vapor pressure values in the metastable liquid region, while a relative abundance of data is available in the stable one. However, in both cases, only qualitative considerations can be made about their agreement, considering that very poor information about the uncertainty analysis is reported in the corresponding works.

For example, Pupezin *et al.*[2] assigns an uncertainty of $\pm 0.0003 \cdot \ln(p_{H2O}/p_{D2O})_{liquid}$ units to the measured vapor pressure isotope effect (VPIE), from which it is possible to presume an uncertainty of about 150 mPa at 273 K to about 380 mPa at 286 K; Bottomley [6] makes reference to the equipment accuracy of determining the pressure and the temperature of 133 mPa and 1 mK respectively; Kraus and Greer [7] report a reproducibility of their data between 4 Pa at 258 K and 1.33 Pa at 277 K; Jakli and Van Hook [5] state an uncertainty on D_2O pressure of about 0.03 % above 293 K, and not quite as well below 293 K; Jakli and Illy [4] refer an experimental precision in the measurement of the pressure of about 0.2 %÷0.3 %; Markò *et al.*[15] state an uncertainty on D_2O vapor pressure of 0.2 Pa at the triple point (276.97 K).

In the stable liquid region, most of data deviates from the reference equation and the present results by few pascal, while in the metastable region a large scattering of Kraus and Greer's data can be observed. A better agreement is noticed among the IAPWS R16-17 formulation, present data and those of Bottomley [6].

In Figure 5 the measured saturation vapor pressure is also compared to the saturation vapor pressure formulations [2-5, 16-21] available in the literature from the 1970s to the author's knowledge. Formulations taken into account are listed in Table IV. All data are plotted as pressure relative difference, $100x\Delta p_{sat}/p_{sat}$, in percent with respect to IAPWS R16-17 formulation. For clarity, the expanded ($k = 2$) combined uncertainty bars are shown only for the first run of the experimental data.

Figure 5. Comparison between saturation vapor pressure measurements with different saturation vapor pressure formulations and their extrapolations. All data are reported as percentage saturation pressure difference, $100\times\Delta p_{sat}/p_{sat}$, with respect to the IAPWS R16-17 formulation, used as reference, versus the temperature T. Only experimental values of the first run of this work are shown with the expanded ($k = 2$) combined measurement uncertainty for the sake of clarity.

Table IV. List of the saturation vapor pressure formulations compared with the experimental data of this work and their temperature range of validity.

Author	*Ref*	*Year*	*Validity range of the formulation*
Pupezin *et al.*	[2]	1972	270 K < T < 373 K
Besley and Bottomley	[3]	1973	278 K < T < 298 K
Jancso and Van Hook	[17]	1974	268 K < T < 623 K
Tanishita *et al.*	[18]	1974	277 K < T < 644 K
Hill and MacMillan	[19]	1979	277 K < T < 644 K
Jakli and Illy	[4]	1980	278 K < T < 363 K
Jakli and Van Hook	[5]	1981	283 K < T < 363 K
Matsunaga and Nagashima	[20]	1987	277 K < T < 644 K
Harvey and Lemmon	[16]	2002	277 K < T < 644 K
Herrig *et al.*	[21]	2018	277 K < T < 644 K

Figure 5 highlights an overall agreement between the experimental data and most of the literature formulations, including the reference, despite many of them are being extrapolated in the region below D_2O melting point which is beyond their specific range of validity. The formulation provided by Tanishita *et al.* [18] strongly deviates from the reference IAPWS R16-17 formulation [21, 23] over the whole temperature range, while that one provided by Besley and Bottomley [3] diverges below 270 K.

4. Conclusions

Saturation vapor pressure measurements of liquid heavy water were carried out at INRIM in a broad temperature range from 256 K to 286 K, including a part of the supercooled region, more precisely a range of 21 K. A measurement method and an experimental apparatus already validated by the work of Beltramino *et al.* [24] for supercooled ordinary water were used.

Heavy water sample was provided by a commercial producer with a specified purity level of 99.9 atomic % D. Great care was taken to preserve the purity during the transferring from the reservoir cell to the sample cell. Pressure and temperature measurements were carried out with sensors calibrated against INRIM reference standards, ensuring the traceability of saturation vapor pressure measurements. Experimental pressure measurements were estimated with a backward extrapolation method and corrected for the hydrostatic head, the thermal transpiration effect and the purity of the water sample. A detailed uncertainty analysis was carried out, obtaining an expanded ($k = 2$) combined uncertainty of saturation vapor pressure measurements that varies from 0.23 Pa at 256 K to 0.85 Pa at 286 K.

The results compare favorably with many saturation vapor pressure formulations [2-5, 16-21], including the last EOS adopted by IAPWS [21, 23], both in the stable liquid region and in the metastable liquid one, while a meaningful comparison with past experimental data results difficult because of the limited information about their uncertainty analysis.

The experimental data obtained in this work underpin a possible range extension down to 256 K of the D_2O saturation vapor pressure formulations and partially meet the pressing requirement for a further range extension to even lower temperatures, a region not yet explored for heavy liquid water.

6. References

[1]   S.A. Wallace, J.N. Mathur, B.J. Allen, Med. Phys. **22** (1995) 585-590, https://doi.org/10.1118/1.597585.

[2]   J. Pupezin, G.Jakli, G. Jancso, W.A. Van Hook, J. Phys. Chem. **76**, 5 (1972) 743-762, https://doi.org/10.1021/j100649a025.

[3]   L. Besley, G.A. Bottomley, J. Chem. Thermodynamics **5**, 3 (1973) 397-410, https://doi.org/10.1016/S0021-9614(73)80031-X.

[4]   G. Jakli, H. Illy, KFKI-1980-15 (1980).

[5]   G. Jakli, W.A. Van Hook, J. Chem. Eng. Data **26**, 3 (1981) 243-245, https://doi.org/10.1021/je00025a004.

[6]   G.A. Bottomley, Austr. J. Chem. **31**, 6 (1978) 1177-1180, https://doi.org/10.1071/CH9781177.

[7]   G.F. Kraus, S.C. Greer, J. Phys. Chem. **88**, 20 (1984) 4781-4785, https://doi.org/10.1021/j150664a067.

[8]   G.N. Lewis, R.T. MacDonald, J. Am. Chem. Soc. **55**, 7 (1933) 3057-3059, https://doi.org/10.1021/ja01334a515.

[9]   F.T. Miles, A.W.C. Menzies, J. Am. Chem. Soc. **58**, 7 (1936) 1067-1069, https://doi.org/10.1021/ja01298a001.

[10] K. Niwa, E. Shimazaki, J. Chem. Soc. Jpn. **60**, (1939) 985.

[11] G.D. Oliver, J.W. Grisard, J. Am. Chem. Soc. **78**, 3 (1956) 561-563, https://doi.org/10.1021/ja01584a013.

[12] C.T. Liu, W.T. Lindsay, J. Chem. Eng. Data **15**, 4 (1970) 510-513, https://doi.org/10.1021/je60047a015.

[13] G. Jakli, L. Markò, ACH Models Chem. **132**, (1995) 226.

[14] K. Zieborak, Z. Phys. Chem. **231** (1966) 248-258, https://doi.org/10.1515/zpch-196623129.

[15] L. Markò, G. Jakli, G. Jancso, J. Chem. Thermodyn. **21**, 4 (1989) 437-441, https://doi.org/10.1016/0021-9614(89)90146-8.

[16] A.H. Harvey, E.W. Lemmon, J. Phys. Chem. Ref. Data **31**, 1 (2002) 173-181, https://doi.org/10.1063/1.1430231.

[17] G. Jancso, W.A. Van Hook, Chem. Rev. **74**, 6 (1974) 689-750 https://doi.org/10.1021/cr60292a004.

[18] I. Tanishita, K. Watanabe, M. Uematsu and K. Eguchi, Proc. 8th Int. Conf. Prop. Steam, Paper VI-4 (1974).

[19] P.G. Hill, R.D.C. MacMillan, Ind. Eng. Chem. Fundamen. **18**, 4 (1979) 412-415, https://doi.org/10.1021/i160072a020.

[20] N. Matsunaga, A. Nagashima, Int. J. of Thermophys. **8**, (1987) 681-694, https://doi.org/10.1007/BF00500788.

[21] S. Herrig, M. Thol, A.H. Harvey and E.W. Lemmon, J. Phys. Chem. Ref. Data **47**, 4 (2018) 043102-1 - 043102-42, https://doi.org/10.1063/1.5053993.

[22] P.G. Hill, R.D.C. MacMillan and V. Lee, J. Phys. Chem. Ref. Data **11**, 1 (1982) 1-14, https://doi.org/10.1063/1.555661.

[23] IAPWS, Revised Release on the IAPWS Formulation 2017 for the Thermodynamic Properties of Heavy Water (2018), http://www.iapws.org/relguide/Heavy-2018.pdf.

[24] G. Beltramino, L. Rosso, R. Cuccaro, S. Tabandeh, D. Smorgon and V. Fernicola, J. Chem. Thermodyn. **141** (2020) 105944, https://doi.org/10.1016/j.jct.2019.105944.

[25] IAPWS, Guideline on Thermodynamic Properties of Supercooled Water (2015), http://www.iapws.org/relguide/Supercooled.pdf.